NANOSTRUCTURED MESOPOROUS SILICA FILMS

M. CLARA GONÇALVES*, GEORGE S. ATTARD
Department of Chemistry, Southampton University, Southampton SO17 1BJ, UK.
** Departamento de Engenharia de Materiais, IST, Universidade Técnica de Lisboa, Av. Rovisco Pais, 1000 Lisboa, Portugal*

ABSTRACT

The lyotropic liquid crystalline phases of surfactants have been used as templates for the synthesis of mesoporous nanostructured materials. To achieve direct templating by liquid crystalline phases, surfactant concentrations in excess of 30 wt% in water are used. In the case of silicas and metallosilicates the materials are obtained as monolithic objects with typical dimensions greater than 5 mm. Here we report on the processing of thin films of nanostructured mesoporous silicas by dip coating from mixtures that contain high surfactant concentrations. We find that the addition of methanol to the reaction mixture facilitates the formation of uniform, crack-free films. By altering the surfactant to water ratio we were able to obtain films that had micellar cubic (I_1), normal topology hexagonal (H_I), or lamellar (L_α) organization. Calcination of these films afforded adherent films that in most cases retained the long-ranged architecture of the liquid crystalline phase. The methanol concentration of the dip-coating mixture was observed to have no effect on the structural parameters of the resulting calcined films.

1. Introduction

The seminal work conducted by researchers at the Mobil Oil Corporation in the early 1990's on the synthesis of mesoporous silicates has led to a number of syntheses in which surfactants are used as templates [1-4]. Typically syntheses of mesoporous oxides employ surfactant concentrations less than 7 wt% with respect to the water content of the reaction mixture. The materials produced by using surfactant templates are characterized by a regular system of uniformly sized pores and extremely high surface areas (900-1500 m^2g^{-1} in the case of silica). In most cases, mesoporous materials are obtained as fine powders as a consequence of the biphasic nature of the reaction medium. However, it has been shown recently that reaction mixtures with low surfactant concentrations can be used to process fibers and supported thin films [5-7].
In 1995 we reported the use of homogeneous (i.e. monophasic) lyotropic liquid crystalline phases as templates for the synthesis of silicas and metallosilicates from sol-gel precursors such as tetramethyl orthosilicate (TMOS) [8]. To achieve homogeneous phases we used surfactant concentrations that were higher than 30 wt%. One of the advantages of using homogenous phases as templates is that the nano-architecture of the

Y.G. Gogotsi and I.V. Uvarova (eds.),
Nanostructured Materials and Coatings for Biomedical and Sensor Applications, 159-168.

reaction mixture is retained throughout the condensation and gelation process and hence the nanostructure of the material can be determined *a priori*. For example, the synthesis of silica in the normal topology hexagonal phase (H_I) of a surfactant leads to silica with cylindrical pores of uniform diameter and indefinite length disposed on a long-ranged hexagonal lattice. This silica is denoted by H_I-SiO_2 to show that its nano-architecture is derived from that of the H_I phase. The diameters of the cylindrical pores are controlled by altering the length of the hydrocarbon chain of the surfactant or by adding hydrophobic compounds such as *n*-dodecane or mesitylene. I_1-SiO_2, Ia3d-SiO_2 and L_α-SiO_2 have been obtained from the corresponding phases [9]. A consequence of using homogeneous lyotropic phases as templates is that the resulting calcined materials are monolithic in nature but have the high surface areas associated with mesoporous silicas. Although the production of thin films of mesoporous silicas by dip-coating from reaction mixtures containing low surfactant concentrations has been reported, we were interested in the ability to process analogous films from the reaction mixtures that are used to produce materials from homogeneous liquid crystalline phases. Thin films of mesoporous nanostructured silica are of interest for a range of applications, in particular integrated sensors. Here we report on studies of the relationships between the composition of the reactive mixture and the nature and quality of the films that can be obtained by dip-coating.

The reaction mixtures we employed consisted of Brij56™ as the non-ionic surfactant, water acidified to pH 2 with HCl and TMOS as the silica precursor. At pH 2 the hydrolysis and subsequent condensation of the TMOS are decoupled temporally, with hydrolysis occurring in a few minutes with condensation taking between 6 and 12 hours. Upon hydrolysis of the TMOS methanol is released which prevents the formation of a liquid crystalline phase in the preparation of monolithic mesporous silica. However, the rheology of the liquid crystalline phases is such that it is impossible to process them into thin films by dip coating. Hence in our experiments the methanol released by the hydrolysis of the TMOS was not removed. Indeed we chose to add differing amounts of methanol to investigate its effect on the quality of the films and the nature and regularity of the nanostructure.

2. Experimental

2.1. MATERIALS

The silica precursor, tetramethyl orthosilicate (TMOS), $Si(OCH_3)_4$, and the non-ionic surfactant Brij56™ were purchased from Aldrich Chemical Co. and were used as received. The pH of the water used in the dip-coating mixtures was adjusted to pH 2 by using hydrochloric acid.

2.2. TEMPLATING MIXTURES

The procedure used to prepare the mesoporous silica films was based on the method described by Attard et. al. [8]. To determine the effect of methanol on the dip-coating process and on the properties of the resulting silica films, 2.5 g of methanol was added to each of the compositions following the first dip coating. After each subsequent dip-coating further aliquots of 2.5 g of methanol were added to the mixture. Thus for each

composition, films were produced from mixtures containing 7.5 g, 10.0 g, 12.5 g and 15.0 g of methanol in batch mixtures of 6 g of Brij56™ / TMOS / acidified water. All the films were processed within 15 minutes from adding the acidified water to the initial Brij56™/TMOS/methanol mixtures.

Two series of mixtures were investigated. In Series 1 the mass ratio of TMOS to Brij56™ was kept equal to 9:5. Varying amounts of acidified water were added to this mixture to produce the component mixtures of this Series. In Series 2 the mass ratio of acidified water to Brij56™ was kept constant and equal 1:1. Varying amounts of TMOS were added to this mixture to make the components of this Series. Details of the compositions of the mixtures we investigated are shown in Table 1.

Table 1. Compositions of mixtures employed to fabricate nanostructured films.

Brij56™/ water (wt%)	Brij56™ (g)	TMOS (g)	TMOS (mole)	0.5 M HCl (g)	Water (mole)	R (molar ratio)	Total mass (g)
1d) 1	0.060	0.108	7.08×10^{-4}	5.832	0.3270	461.86	6
1e) 5	0.276	0.498	3.27×10^{-3}	5.232	0.2930	89.60	6
1f) 10	0.510	0.918	6.02×10^{-3}	4.578	0.2560	42.52	6
1g) 20	0.882	1.590	1.04×10^{-2}	3.528	0.1980	19.04	6
1h) 30	1.170	2.106	1.38×10^{-2}	2.730	0.1530	11.09	6
1i) 40	1.398	2.514	1.65×10^{-2}	2.094	0.1170	7.09	6
1j) 50	1.578	2.844	1.86×10^{-2}	1.578	0.0890	4.75	6
1k) 60	1.728	3.114	2.04×10^{-2}	1.152	0.0645	3.16	6
1l) 70	1.860	3.348	2.20×10^{-2}	0.798	0.0447	2.03	6
1m) 80	1.968	3.540	2.32×10^{-2}	0.492	0.0276	1.19	6

TMOS:Brij56™ (wt%)	Brij56™ (g)	TMOS (g)	TMOS (mole)	0.5 M HCl (g)	Water (mole)	R (molar ratio)	Total mass (g)
2a) 1.00	1.998	1.998	1.31×10^{-2}	1.998	0.112	8.549	6
2b) 1.40	1.764	2.472	1.62×10^{-2}	1.764	0.099	6.111	6
1j) 1.80	1.578	2.844	1.86×10^{-2}	1.578	0.088	4.750	6
2c) 2.20	1.428	3.144	2.10×10^{-2}	1.428	0.080	3.809	6
2d) 2.60	1.302	3.390	2.20×10^{-2}	1.302	0.073	3.318	6
2e) 3.00	1.200	3.600	2.36×10^{-2}	1.200	0.067	2.839	6
2f) 4.00	1.002	4.002	2.63×10^{-2}	1.002	0.056	2.129	6

2.3. DIP-COATING

Microscope slides (7.5 cm × 2.5 cm) were used as substrates for dip-coating. These were degreased with a laboratory detergent, rinsed repeatedly first with distilled water then with acetone, and subsequently dried in an oven at 50°C. To dip-coat a film the slide was immersed to a depth of ca 3.5 cm into the reaction mixture, allowed to stand for 1 minute and then withdrawn at a speed of 0.1 cm s^{-1}. The films were cured in an oven at 40°C for 5 days. Surfactant was removed from the films by calcination in a tube furnace. The films were heated to 450°C under nitrogen for 8 h followed by oxygen for 12 h.

2.4. FILM CHARACTERIZATION

The structures of the as deposited cured films were investigated by polarized light microscopy and by low angle X-ray diffraction (XRD). The structures of the calcined

films were investigated by polarized light microscopy, low angle X-ray diffraction and transmission electron microscopy (TEM). The macroscopic morphology and quality of the calcined films were also assessed by scanning electron micrscopy (SEM). The optical anisotropy of the as deposited cured films and the calcined films was investigated by polarized light microscopy using an Olympus BH-2 polarized light microscope.

Scanning electron microscopy studies were carried out using a JEOL JSM-6400 Analytical Scanning Electron Microscope operating at a voltage of 20 kV. Transmission electron microscopy investigations were conducted with a JEOL 2000FX Transmission Electron Microscope operating at a voltage of 200 kV. Samples for TEM were ground and suspended in water. The suspensions were sonicated for 25 min and then applied to a 400 mesh carbon-coated copper grid.

Low-angle X-ray diffractograms were recorded over the range ~ 0.7 to ~ 3.0 2θ degrees (Cu K_α radiation) using a Siemens D5000 diffractometer.

3. Results and Discussion

The results from XRD and TEM studies on the dip-coated films produced from **Series 1** are summarized in Table 2, for the most representative samples. Data obtained from the calcined films are shown in the shaded rows to distinguish them from the data pertaining to the as-synthesized cured films.

In the templating mixtures in **Series 1** the ratio of Brij56™ to TMOS was kept constant and the only variables were the amounts of water and methanol present. Mixture **1d** contained the highest amount of water while mixture **1m** the lowest. Table 2 shows that by decreasing the water content of the templating mixture, films having micellar cubic (I_1), hexagonal (H_I) and lamellar (L_α) nano-architectures could be obtained irrespective of the amount of methanol present.

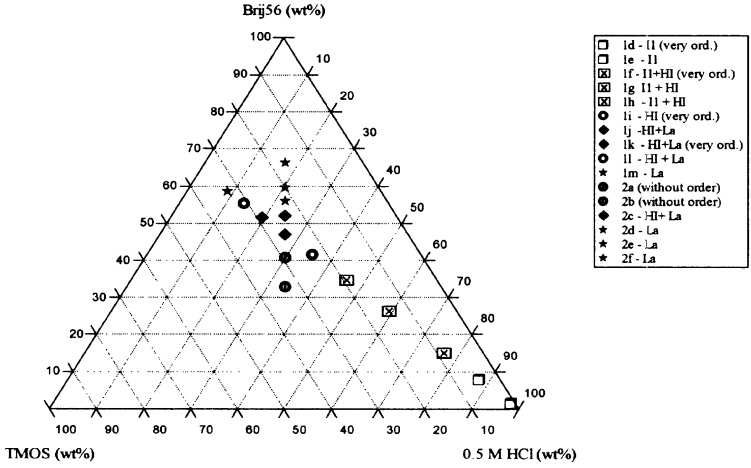

Figure 1. Map of the nanostructures of the calcined films on a ternary phase diagram.

The final nanostructures of the calcined films prepared from **Series 1** and **Series 2** are mapped onto a ternary phase diagram in Figure 1.

Representative X-ray diffraction data obtained from **Series 1** films prepared from the precursor mixtures with 15,0 g of methanol addition, are illustrated in Figures 2. In the case of the monophasic systems, the X-ray data suggest that the lattice parameters of the as synthesized cured films fall in the range 5.5 nm to 4.8 nm. The data from the as synthesized films that are in an homogeneous H_I phase, and those in an homogeneous L_α phase, suggest that the wall-to-wall distance decreases from ~ 6 nm to ~ 5.2 nm on traversing the phase diagram. Since it was not possible to assign the structure of the micellar cubic phase because of insufficient X-ray reflections, we are unable to determine whether the wall-to-wall distance in the I_1 phase is larger than that of the H_I phase. However, both the decrease in this parameter on going from the H_I to the L_α phase, as well as the magnitude of the change, are comparable with previous observations on non-ionic surfactants.

(a)

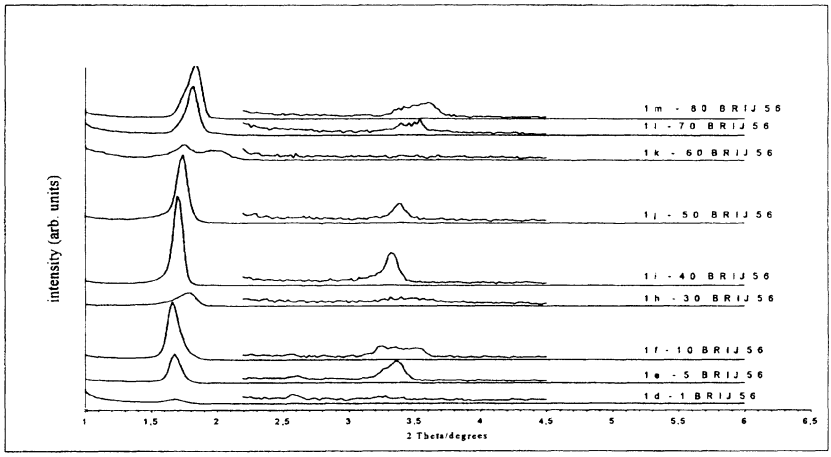

(b)

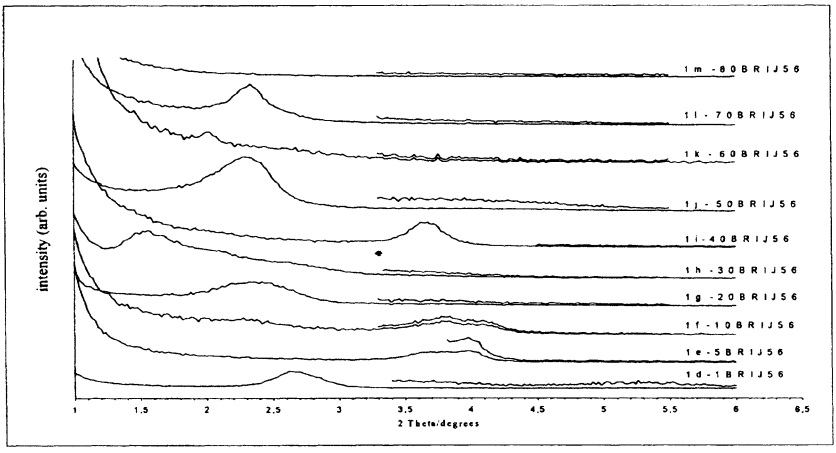

Figure 2. Small angle X-ray diffractograms obtained from dip-coated films processed from the mixtures in **Series 1**, for 15,0 g of methanol addition. (a) as synthesized films, (b) calcined films.

Table 2. Summary of low angle X-ray diffraction data and observations from TEM for films prepared from mixtures of **Series 1**.

Series label	Conc. of Brij56 /wt%	MeOH addition / g	Position of first reflect. /2θ ±0.1°	Peak width at half height of first reflect. /°	d spacing for first reflect. /nm	Further peaks and indexing /2θ (± 0.1°)	Structure assignment	Pore to pore distance from XRD / nm (± 0.5 nm)	Pore-pore distance from TEM /nm (± 0.5 nm)
1d	1	7.5	1.66	0.15	5.32	2.62 , 3.30	I_1 (Fd3m)	-	
			2.56	0.35	3.45	3.00 , 3.64	I_1 (Fd3m)	-	
		15.0	1.70	0.19	5.19	2.60 , 3.30	I_1 (Fd3m)	-	
			2.70	0.42	3.27	5.28	I_1 (Fd3m)		
1f	10	7.5	1.65	0.11	5.35	2.60 , 3.24	Biphasic	-	
			2.06	0.36	4.29	4.0	Biphasic	-	
		15.0	1.68	0.11	5.25	2.60 , 3.36	Biphasic	-	
			2.30	0.29	3.84	3.84	Biphasic	-	a=3.87 , d=4.33
1h	30	7.5	1.76	0.19	5.02	3.42	Biphasic	-	
			2.54	0.66	3.48	-	-	-	d_1=3.01 , d_2=4.37
		15.0	1.80	0.19	4.90	3.5(200)	Biphasic	-	
			1.58	0.36	5.59				d_1=2.07 , d_2=520
1l	40	7.5	1.70	0.24	5.19	3.28	H_1	5.99	
			-	-	-	-	-	-	a=3.75 , d=4.13
		15.0	1.72	0.09	5.13	3.34	H_1	5.92	
			3.69	0.28	2.39			2.76	a=3.75 , d=4.26
1j	50	7.5	1.76	0.20	5.02	3.44	Biphasic	-	
			2.01	0.36	4.39	4.08	Biphasic	-	
		15.0	1.76	0.10	5.02	3.4	Biphasic	-	
			2.28	0.52	3.87	4.26	Biphasic	-	d=4.43
1l	70	7.5	1.92	0.29	4.60	3.18 , 3.58	L_α+Phase	4.60	
			2.43	0.38	3.63	4.76	L_α+Phase	3.63	
		15.0	1.82	0.09	4.85	3.52	L_α+Phase	4.85	
			2.34	0.29	3.77			3.77	d_1=4.12 , d_2=3.81

Calcination of the films in **Series 1** leads to pure silica films that retain the nano-architectures of the cured films. Representative transmission electron micrographs are shown in Figure 3. A significant contraction in the lattice parameter determined by XRD is observed following calcination. The contraction is typically a factor of 0.7 for the I_1 materials, 0.8 for the H_I materials and 0.8 for the L_α materials. If this shrinkage is of equal magnitude along each of the three cartesian co-ordinates, then it would correspond to the volume of the calcined film shrinking by nearly a factor of 3 compared with the as synthesized film. This magnitude of shrinkage is comparable with our previous observations on H_I-SiO_2 and is significantly lower than the volume shrinkage observed typically with sol-gel synthesis of silica monoliths [8, 10].
The presence of methanol in the precursor mixtures of **Series 1** does not appear to affect the lattice parameters of the as synthesized films, at least within the limits of experimental reproducibility. By contrast the calcined films do show a significant decrease in the lattice parameter as a function of increasing methanol content. For example, in the case of the calcined I1 films the lattice parameter decreases from 3.5 nm for films prepared with the lowest methanol addition of 7.5 g, to 2.5 nm for films prepared with 15g methanol. A similar decrease is observed for the calcined H_I films, but the lattice parameter for the calcined L_α films is essentially unaffected by methanol concentration

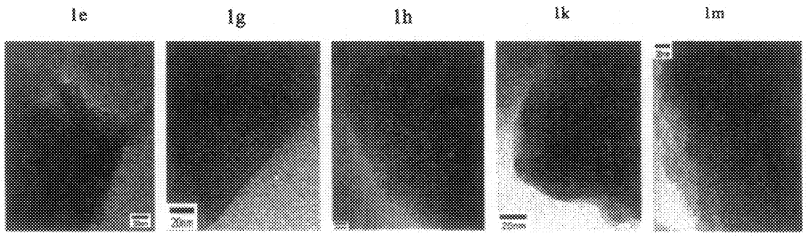

Figure 3. Transmission electron micrographs obtained from calcined dip-coated films processed from the mixtures in **Series 1**.

In the case of the dip-coated films the birefringent optical textures were not sufficiently resolved to allow an unambiguous assignment of the nano-architecture. The only significant observation that we were able to make was that films that were biphasic either in their as synthesized state or following calcination were more likely to develop cracks after calcination.
In the templating mixtures of **Series 2** the surfactant to water ratio is constant, but the amount of TMOS, as well as methanol, is varied. Mixture **2a** has the highest water:TMOS molar ratio (8.6) while mixture **2f** has the lowest (2.1). Of all the compositions investigated, mixture **2c** is closest to the stoichiometric composition for the hydrolysis of TMOS (1 mole equivalent TMOS to 3.8 mole equivalent water). In the as synthesized and cured films of **Series 2** we found that increasing the amount of TMOS in the precursor mixture lead to the progressive formation of a lamellar nanostructure; this is preceded by a broad biphasic domain.
X-ray diffractograms for both as synthesized and calcined films were obtained from reaction mixture **Series 2.** For the as synthesized films the lattice parameter does not

appear to change as the amount of TMOS is increased for the single phase systems. This observation applies irrespective of the amount of methanol in the templating mixture. By contrast, calcined films with an L_α nanostructure do show some dependence of their lattice parameters on the amount of methanol. For example, the lattice parameter for mixture **2m** and with 15 g of methanol is 3.1 nm while for the lowest methanol addition 7.5 g is 3.6 nm. Overall the lattice parameter decreases by a factor of ca 0.7 following calcination.

As in the case of **Series 1**, we found that biphasic films from **Series 2** were more likely to produce cracked films following calcination than were homogeneous films. This observation suggests that the polycrystalline domain morphology of the biphasic films could lead to unequal shrinkage and the build-up of stress that leads to fracturing and delamination during calcination.

It is observed from SEM images that the thickness of our films varied in the range 300 nm to 600 nm. Previous work on dip-coated sol-gel mixtures suggests that crack free films should be achievable with ease provided the cured film thickness is less than ca 1μm [11]. In these cases shrinkage tends to occur primarily in the direction orthogonal to the film plane. In both series the thickness of the calcined films was found to decrease in proportion to the amount of methanol present in the reaction mixture. The thickness shrinkage is typically a factor of 0.5, decreasing from a typical value of 1.1 μm for the lowest methanol addition to 0.65 μm, for 15.0g of methanol contend. The uniformity of the films was observed to improve significantly as a function of the methanol concentration of the dipping solution.

The widths of the XRD peaks, illustrated in Table 2 for the most significant samples of Series 1, provide qualitative insights into how the regularity of the mesoporous architecture is affected by the composition of the precursor mixture. In the case of **Series 1**, there was very little change in the diffraction peak width of the as synthesized films on going from the homogeneous I_1 phase, through the H_1 phase and into the L_α phase. Similarly, there were no significant changes in peak width between samples with different methanol concentrations. The calcined films from **Series 1** showed an increase in the peak width compared with the as synthesized films. This is consistent with previous observations and indicates that calcination introduces a degree of disorder in the structure, presumably as a consequence of the significant contraction in volume [8]. We did not observe any systematic changes in peak width as a function of methanol concentration or phase architecture. The films in **Series 2** showed similar behavior to those in Series 1. We did however note that in the case of the samples templated in a lamellar phase, there seemed to be a bigger increase in the peak width following calcination than was the case for films templated in either the H_1 or I_1 phases.

Previous studies on mesoporous silica films prepared by dip-coating from precursor solutions that contained low surfactant concentrations (<7 wt%) showed that the mesoporous nano-architecture of a dip-coated film will often vary across the film [12]. Although at a molecular and mesoscopic level dip-coating involves a number of complex and poorly understood processes, it is clear from earlier work that the rapid evaporation of water and methanol immediately following film deposition can lead to severe concentration gradients across the film [12]. We expect this to be the case for most of our films, but without any direct evidence. However, the observation that the overall film quality, as judged by optical microscopy, improves with increasing methanol concentration provides some support for this expectation. Furthermore, the apparent insensitivity of the lattice parameters in the as synthesized cured films to the

methanol concentration of the precursor mixture is a significant observation as it implies that the final structure adopted by the films is essentially determined by the relative amounts of surfactant, TMOS and water. In other words our data suggest that the methanol plays no role in the templating process; its presence ensures that the solution has the appropriate rheology for dip-coating. The main consequences of having methanol in the precursor mixture are a more dramatic decrease in the lattice parameters upon calcination. Presumably this reflects the lower density of the incipient silica formed in the presence of large amounts of methanol. When the film forms the methanol flash-evaporates from the film, however, the films retain the structure of the templating lyotropic phase. In most cases there is further continuity with the structure of the calcined material.

4. Conclusions

We have demonstrated that it is feasible to use precursor mixtures that contain high surfactant concentrations to dip-coat thin silica films onto glass slides. The macroscopic uniformity of the films appears to improve when methanol is added to the mixture, although methanol plays no role in the templating process. Our data indicate that amount of methanol in the dip coating mixture has little effect on the structural parameters of the as synthesized films, but does lead to more significant volume shrinkage on calcination.

5. Acknowledgements

This work was supported by the Engineering & Physical Sciences Research Council of the UK. The authors would like to thank Dr. Barbara Cressey for her help with the TEM. M. Clara Gonçalves would like to thank Fundação para a Ciência e a Tecnologia, who supported the work by a grant FMRH/BSAB/203/0.

6. References

1. Beck, J.S., Vartuli, J.C., Roth, W.J., Leonowicz, M.E., Kresge, C.T., Schmitt, K.D., Chu, C.T.-W., Olson, D.H., Sheppard, E.W., McCullen, S.B., Higins, J.B., and Schlenker, J.L. (1992), *J. Am. Chem. Soc.* **114**, 10834.
2. Kresge, C.T., Leonowicz, M.E., Roth, W.J., Vartuli, J.C., and Beck, J.S. (1992), *Nature* **359**, 710.
3. Bagshaw, S.A., and Pinnavaia, T.J. (1996), *Angew. Chem. Intl. Ed. Engl.* **35**, 1102.
4. Zhao, D., Huo, Q., Feng, J., Chmelka, B.F., and Stucky, G.D. (1998), *J. Am. Chem. Soc.* **120**, 6024.
5. Bruinsma, P.J., Kim, A.Y., Liu, J., and Baskaran, S. (1997), *Chem. Mater.* **9**, 2507.
6. Lu, Y.F., Ganguli, R., Drewien, C.A., Anderson, M.T., Brinker, C.J., Gong, W.L., Guo, Y.X., Soyez, H., Dunn, B., Huang, M.H., and Zink, J.I. (1997), *Nature* **389**, 364.
7. Lu, Y.F., Yang, Y., Sellinger, A., Lu, M.C., Huang, J.M., Fan, H.Y., Haddad, R., Lopez, G., Burns, A.R., Sasaki, D.Y., Shelnut, J., and Brinker, C.J. (2001), *Nature* **410**, 913.
8. Attard, G.S., Glyde, J.C., and Goltner, C.G. (1995), *Nature* **378**, 366.
9. Attard, G.S., Edgar, M., and Göltner, C.G. (1998), *Acta Materialia* **46**, 751.
10. Coleman, N.R.B., and Attard, G.S. (2001), *Micropor. 7 Mesopor. Matls.* **44-45**, 73.
11. Brinker, C.J., Hurd, A.J., Frye, G.C., Ward, K.J., and Ashley, C.S. (1990), *J. Non-Crystalline Solids* **121**, 294.
12. Brinker, C.J., Hurd, A.J., Schunk, P.R., Frye, G.C., and Ashley, C.S. (1992), *J. Non-Crystalline Solids* **147&148**, 424.